Magnetic Resonance Imaging of the Normal Equine Larynx

by

Cortney Erik Henderson, DVM

Thesis submitted to the faculty of Virginia Polytechnic Institute and State University in partial fulfillment of the requirements for the degree of

Master of Science

In

Biomedical and Veterinary Sciences

Kenneth E. Sullins, Chairman

Nathaniel A. White II

Jill McCutcheon

C. Douglas Phillips

June 22, 2006

Leesburg, Virginia

Keywords: magnetic resonance imaging, MRI, larynx, horse, respiratory

Magnetic Resonance Imaging of the Normal Equine Larynx

by

Cortney Erik Henderson, DVM

Committee Chairman: Kenneth E. Sullins, DVM, MS
Diplomate American College of Veterinary Surgeons
Professor of Equine Surgery

(ABSTRACT)

A study was performed to establish the appearance of normal equine laryngeal cartilages using magnetic resonance imaging. Specimens were acquired from clinically normal horses that were euthanized for reasons other than respiratory disease. Three *in situ* and 5 *ex vivo* larynges were imaged using a 0.3 Tesla system. Images were obtained in the transverse plane using T1-weighted 3D spin echo, T2-weighted 3D spin echo, T2-weighted gradient echo, short tau inversion recovery (STIR), and proton density spin echo sequences. Five *ex vivo* larynges were also imaged in the transverse plane using a 1.5 Tesla system, sequences included T1-weighted 3D spin echo, T2-weighted 3D turbo-spin echo, turbo inversion recovery (TIRM), and proton density spin echo sequences. A frozen gross laryngeal specimen was sliced in 5-mm transverse sections for comparison to the MR images. Excellent correlation was found between MR images and the gross transverse sections. Successful imaging was accomplished using both imaging systems; however, the 1.5 Tesla system yielded superior image resolution. The 0.3 Tesla imaging system would accommodate the intact equine head, which was not possible using the 1.5 Tesla MRI system. The internal morphology of the laryngeal cartilages was clearly identified in all imaging sequences obtained. Cartilages were found to differ in signal intensity

based on the tissue composition and imaging sequences performed. MRI was determined to be a useful imaging modality for evaluating the cartilage morphology of the equine larynx. Further investigation is required to document pathologic morphology.

GRANT INFORMATION

This research effort was funded by the Patricia Bonsall Stuart Equine Research Award.

DEDICATED TO

Cara Henderson

My wife, who has provided never-ending support throughout our marriage and my career.

Eddie and Sandy Henderson

My father and mother, who gave me the opportunity to pursue my interest in veterinary medicine.

ACKNOWLEDGEMENTS

Kenneth E. Sullins – my research advisor, for his help and guidance with the MRI research study, assorted publications and the masters program.

Nathaniel A. White – for help and guidance through the residency program.

Jill McCutcheon – for guidance through the masters program and with thesis preparation requirements.

C. Douglas Phillips – for guidance and imaging feasibility for the masters research project.

Carolyn Smith - for MRI technical assistance.

John Christopher - for MRI technical assistance.

TABLE OF CONTENTS

LIST OF FIGURES

Page

LIST OF ABBREVIATIONS

MRI = magnetic resonance imaging

MR = magnetic resonance

TIRM = turbo inversion recovery

IR = inversion recovery

mm = millimeter

RF = radio-frequency

TR = repetition time

TE = echo time

STIR = short tau inversion recovery

CT = computed tomography

3D = three dimensional

ms = millisecond

cm = centimeter

INTRODUCTION

Disease of the equine larynx limits performance by causing exercise intolerance and abnormal upper respiratory noise. Traditional evaluation of the equine larynx is based on physical examination, upper airway endoscopy, and radiography. While these diagnostic tools contribute to the diagnosis of certain laryngeal disorders, the majority of the structure of the laryngeal cartilages cannot be thoroughly evaluated.

Arytenoid chondritis is an acute or chronic, often progressive, bacterial infection that results in thickening of the arytenoid cartilage and airway obstruction. Affected horses experience exercise intolerance and abnormal respiratory noise, and complete airway obstruction is possible in advanced disease states or during strenuous exercise. Traditional treatment is partial arytenoidectomy with the horse under general anesthesia.[1-6] Although racing is possible following arytenoidectomy, the procedure has potential complications and is costly.[1,2,7] An alternative minimally invasive procedure consisting of laser-assisted debridement has been reported in the standing horse if the condition is recognized before permanent arytenoid deformity has occurred.[8,9] Case selection is critical; the diagnostic challenge lies in determining the extent of arytenoid deformity in marginal cases. Endoscopy, radiology, and ultrasound have not completely fulfilled this need. Additional structural diseases of the larynx occur and include palatopharyngeal arch deformity, atrophy and fracture of the laryngeal cartilages, and developmental abnormalities resulting in anatomic alteration of the larynges and surrounding musculature.

Magnetic resonance imaging provides a detailed depiction of the morphology and composition of the tissue based on hydrogen content. Images are produced in gray scale with specific intensities of signal based on the tissue composition. Imaging the cartilage of the equine larynx would aid in deciding whether to debride or remove an arytenoid cartilage.

The intent of this study was to evaluate MRI imaging of the normal equine larynx, so the severity of internal laryngeal cartilage lesions could be determined in clinical cases. My literature review disclosed no prior published reports of MRI of the equine larynx. The magnet configuration and field strength are limited in equine veterinary medicine to equipment that is available in a clinical setting. The purpose of the study was to acquire clinically useful MR images of the normal equine larynx using the 0.3 Tesla permanent C-shaped MRI system that is currently available in clinical practice. Images were also obtained using a 1.5 Tesla superconducting horizontal magnet to depict and describe the normal anatomy. The images acquired were compared with similar slices of gross specimens. We hypothesized that MRI would offer a useful, noninvasive means for evaluation of the morphology of the equine laryngeal cartilages and that the images obtained would correlate well with gross anatomic specimens. A diagnostic standard for normal magnetic resonance imaging will be established to provide a reference for which laryngeal disease may be compared in the future.

LITERATURE REVIEW

THE DEVELOPMENT OF MRI

Current magnetic resonance imaging is based upon the principles of nuclear induction; also known as nuclear magnetic resonance. Bloch and Purcell independently publicized the principle of nuclear induction in 1946 and reported that nuclei of different atoms absorb radio waves of different frequencies.[10,11] They reported that when radio waves were applied to molecules, the orientation of the nuclear moment of the molecules changed based on the radio-wave frequency applied. When the radio-wave frequency was removed from the molecules, nuclear relaxation occurred. Bloch and Purcell demonstrated that the nuclear reorientation due to relaxation could be measured as a voltage difference between terminals of an external electrical circuit.[10,11] As techniques were refined, nuclear magnetic resonance became a spectroscopic technique used in the laboratory setting for the identification of chemical and physical characteristics of specific molecules. Laboratory molecular analysis was the first practical use of magnetic resonance. In 1971, Damadian proposed that nuclear magnetic relaxation times could be used to non-invasively detect disease.[12] Nuclear magnetic relaxation times of neoplastic tissue differed from that of normal tissue and the difference was recordable.[12,13] In 1973, Lauterbur implemented a tri-plane gradient magnetic field for imaging specific areas of the body.[14] This report is thought to be the foundation for current MRI technology and provided a means of spatially localizing the MR signal.

The technique involved magnetic field gradients in the x, y, and z directions applied to the subject, resulting in three dimensional MR signal localization.[14] In 1978, medical imaging

technology was further advanced with the publication of the first human whole-body MRI study. Cross-sectional images of a human thorax depicting tissue structure based on the concentration of tissue water was produced.[15] Since that time, MRI technology has been widely used in medical imaging of the human body. MRI has gradually become more efficient, resulting in constantly improving resolution.

BASIC PHYSICS AND PRINCIPLES OF MRI

The basic principle of magnetic resonance imaging is that hydrogen contained in tissue water emits a signal that is detectable by a magnetic resonance scanner, and permits noninvasive imaging of tissue architecture. Images correspond to slices through the anatomic structure depicted in gray scale; thickness is determined by the operator. Each slice is composed of defined 3-dimensional tissue volumes referred to as voxels, which correspond to small cubic volumes of tissue.[16] The voxel size is variable and may be manipulated to influence the available MR signal, which correlates with the intensity of brightness of a pixel.[17] Images are composed of thousands of pixels which represent the gray scale average MR signal within each tissue voxel. The slice thickness, field of view and the acquisition matrix determine the dimensions of the voxel. Field of view is the square image area that contains the object of interest and is expressed in units of mm^2. It represents the amount of tissue included on each cross sectional image. The smaller the field of view, the higher the image resolution, but the lower the measured MR signal.

The acquisition matrix is a 2-dimensional grid which represents the surface area of the voxels composing the MR image and is expressed as width X height. Because the MR

signal is proportional to the number of protons resonating within each voxel, increasing the size of the voxel will increase the MR signal and improve image acquisition.[18] Therefore, increasing the slice thickness and field of view, or decreasing the imaging matrix will increase the MR signal. Image resolution is the ability to distinguish small objects on MR images and is critical to medical imaging applications. Decreasing the size of the voxel will improve image resolution, but will also decrease the number of available resonating protons, resulting in a decreased signal.[19] Therefore, the available MR signal and image resolution may be improved with manipulation of the imaging parameters.

Variation in the hydrogen content of tissue makes magnetic resonance imaging possible. Magnetism is a property of tissue that results from orbiting electrons. The orbiting electrons cause atoms to have a magnetic moment associated with angular momentum referred to as spin.[16] The spinning protons create a small magnetic field. The concentration of hydrogen atoms in tissue and the large magnetic moment created by the single hydrogen proton make the hydrogen atom extremely sensitive to magnetic resonance. When the tissue is placed within a magnetic field, protons align with or against the applied magnetic field.[16,18,20] At any given time, a slight majority of the tissue protons will be aligned with the applied magnetic field. The aligned position is slightly favored because the nucleus is at a lower energy state, resulting in a net tissue magnetization pointing longitudinally in the direction of the applied magnetic field.[20] The protons wobble as they spin within the applied magnetic field. The rate of proton wobbling is described as precession, and is unique for water protons depending on the frequency of the static magnetic field. Precession is described as Larmor frequency, and is characteristic of the specific tissue being imaged.[16,20] Larmor frequency is the frequency at which the nucleus will absorb

energy to alter its alignment. The stronger the magnetic field, the higher the Larmor frequency. If an RF pulse at the Larmor frequency is applied to the nucleus of an atom, the protons will alter their alignment from the direction of the main magnetic field to the direction opposite the main magnetic field. As the proton tries to realign with the main magnetic field, it will also emit energy at the Larmor frequency. Nuclear resonance is the ability of an atom to absorb energy at the Larmor frequency to alter its alignment. Radio-frequency radiation is applied through an RF coil to individual nuclei at the Larmor frequency and causes the nuclei in a lower energy state to jump into a higher energy state. Exposure of the magnetized tissue to RF radiation at the Larmor frequency causes the net magnetization vector to rotate from a longitudinal position aligned with the applied magnetic field to a distance proportional to the time length of the RF pulse.[20]

The net magnetization vector rotates 90 to 180 degrees from the applied magnetic plane and can be detected by the MRI scanner. The angle that the net magnetization vector rotates at the end of the RF pulse is commonly called the flip angle.[20] The stronger the RF pulse delivered by the coil to the protons, the greater the flip angle for the magnetization. The two most common flip angles in MRI are 90 degrees and 180 degrees, but variable angles are utilized. After the external RF pulse ceases, T1 recovery and T2 decay take place. T1 recovery and T2 decay occur at the same time, but are completely different processes. T1 recovery is the gradual increase in longitudinal magnetization and is referred to as longitudinal relaxation.[16,18] T1 relaxation is a time constant and is the time required for proton alignment to return to 63% of the original longitudinal magnetization.[21] The time between successive RF excitation pulses is repetition time (TR), an imaging parameter which controls the T1 weighting of an image. A short TR maximizes T1 weighting, whereas a long TR minimizes T1 weighting.[19]

T2 decay, or transverse relaxation, is the gradual decrease in transverse magnetization back to an equilibrium of proton alignment.[16,18] As T2 decay occurs, the MR signal "dies out". The decay is expressed as a time constant. The T2 time constant is the time for nuclei spinning perpendicular to the main magnetic field to lose coherence, which results in a loss of transverse magnetization and MRI signal.[17] T2 decay occurs when the transverse magnetization has decreased to 37% of the initial value and is more rapid than T1 recovery.[21] Echo delay time (TE) is the time interval between the RF pulse and the measurement of the first echo that determines the T2 weighting of an image. A short TE minimizes T2 expression, whereas a long TE maximizes T2 weighting.

Each type of tissue has a differing concentration of hydrogen atoms causing different T1 and T2 values. Contrast between various tissues is related to differences in proton resonance within the tissues. Specific imaging parameters selected for an MR scan are referred to as pulse sequences and typically include T1-weighted, T2-weighted, proton density, inversion recovery (IR), and gradient echo.

T1-weighted imaging is considered a short-TR and short-TE sequence. T1-weighted images are especially useful for depicting anatomic detail. Fat, acute hemorrhage, and proteinaceous fluid have high signal intensity (bright).[16] Muscle and most other soft tissue structures are intermediate to low in signal intensity. Fluid composed mostly of water is of relatively low signal when compared to muscle. Cartilage typically has higher signal intensity than muscle and other soft tissue structures.

The T2-weighted sequence has a comparatively long TR and long TE.[16] Fluid produces an especially high signal. T2-weighted images identify tissue pathology well due to the increased fluid content of affected tissue. Muscle and soft tissue structures produce intermediate signal and fat has less signal than on a T1-weighted image.

Proton density sequences are considered an intermediate TR and short TE sequence.[16] Tissue contrast is primarily due to the proton number within specific tissues. The higher the number of protons in a given unit of tissue, the greater the transverse component of magnetization, and the brighter the signal on the proton density contrast image. This sequence provides good anatomic detail, but little overall tissue contrast due to the intermediate weighting. Proton density is particularly useful for evaluation of cartilaginous structures, such as human meniscal pathology.[17] However, this sequence is poor for detection of fluid and bone marrow pathology.

Short tau inversion recovery (STIR) and turbo inversion recovery (TIRM) are T2-weighted fat suppression techniques that result in increased signal intensity from fluid and tissue edema. It is very sensitive in detecting tissue fluid accumulation due to soft tissue pathology and is commonly used in musculoskeletal imaging protocols. The disadvantages of inversion recovery sequences are a longer acquisition time and expression of less anatomical detail.

Gradient echo is a type of pulse sequence generated from free induction decay by an applied bipolar magnetic gradient.[17] The gradient echo is produced by reversing the direction of a magnetic field gradient or by applying balanced pulses of a magnetic field gradient before and after an RF pulse.[16] Gradient echo produces T1 or T2 –weighted images in less time than conventional spin echo techniques. It is particularly useful in imaging ligaments and cartilaginous structures, but is more susceptible to imaging artifacts. Gradient echo tends to produce poor contrast between muscle and other soft tissue structures. The protons within the mineralized matrix of cortical bone are unable to resonate and produce an MR signal; therefore, cortical bone is typically black in all imaging sequences. Disadvantages of gradient echo imaging are compromised anatomic details and artifacts.

EQUINE LARYNGEAL ANATOMY

The larynx is primarily composed of fibroelastic and hyaline cartilage.[22,23] The five laryngeal cartilages are the epiglottic, thyroid, cricoid, and the paired arytenoid cartilages. The most rostral is the epiglottic cartilage which is composed of flexible elastic cartilage.[23,24] The largest is the thyroid cartilage which consists of two lateral hyaline cartilage plates fused along the laryngeal floor.[24] The dorsal, rostral and caudal extremities of the thyroid cartilage articulate with the thyrohyoid bone and cricoid cartilage, respectively.[22] The most caudal is the cricoid cartilage which forms a complete "signet" ring. The cricoid cartilage is joined to the trachea by the cricotracheal ligament. The cricoid cartilage articulates with each arytenoid cartilage via the synovial cricoarytenoid joints and with the dorsocaudal thyroid cartilage via synovial articulations at the lateral facets of the cricoid cartilage. The paired arytenoid cartilages lie on

either side of the laryngeal lumen and contain three processes. The vocal process projects ventrally and serve as the dorsal attachment of the vocal fold. The muscular process projects dorsolaterally for insertion of the cricoarytenoideus dorsalis muscle. The corniculate processes form the laryngeal entrance and the dorso-lateral limits of the glottis. The corniculate process is composed of fibroelastic cartilage and the remaining structure of the arytenoid is composed of hyaline cartilage.[23]

Intrinsic and extrinsic muscles create laryngeal cartilage movement. The extrinsic muscles function as elevators and depressors of the larynx. They include the thyrohyoideus, hyoepiglotticus, and sternothyroideus muscles.[22] The intrinsic muscles control vocal cord tension and the size and shape of the glottis and include the cricothyroideus, cricoarytenoideus dorsalis, cricoarytenoideus lateralis, thyroarytenoideus, and arytenoideus transverses muscles. The cricothyroideus muscle originates from the lateral surface of the thyroid lamina and inserts on the cricoid arch ventral to the cricothyroid joint to tense the vocal fold; it is innervated by the cranial laryngeal nerve.[22] The other intrinsic muscles are innervated by the recurrent laryngeal branch of the vagus nerve. The cricoarytenoideus dorsalis muscle originates from the dorsolateral surface of the cricoid cartilage and inserts on the muscular process of the arytenoid cartilage to abduct the arytenoid cartilages, opening the rima glottidis.[24] The cricoarytenoideus lateralis muscle originates from the rostroventral part of the cricoid arch and inserts on the muscular process of the arytenoid to abduct the arytenoid cartilages, narrowing the rima glottidis. The thyroarytenoideus muscle originates from the thyroid cartilage on the cranial laryngeal floor and inserts on the muscular process and body of the arytenoid cartilage and functions to adjust the tension of the vocal fold. It is divided into two units consisting of the rostral ventricularis

and caudal vocalis muscles. The arytenoideus transverses muscle originates from the muscular process of the arytenoid cartilage, inserts on the median raphe and functions to approximate and stabilize the paired arytenoid cartilages.[22]

The laryngeal ventricle is a diverticulum lined with mucosal tissue which is located dorsal and caudal to the vocal fold, between the arytenoid and thyroid cartilages. The laryngeal ventricles are proposed to act as resonators during vocalization. The vocal folds are soft tissue structures and run caudodorsally from the rostral laryngeal floor to attach on the mid ventral aspect of the body of the arytenoid cartilages. Each vocal fold contains a ligament on the dorsal and ventral free margin for stabilization. The vocal folds can be tensed and relaxed by the cricothyroideus and the thyroarytenoideus muscles during vocalization. The pitch of vocalization is controlled by the thickness, length, and tension of the vocal folds.

MRI OF THE HUMAN LARYNX

Magnetic resonance imaging has been used extensively in the human medical profession. The primary role of MR in human laryngeal imaging is to define the extent of disease, especially neoplastic processes.[25,26] Laryngeal carcinoma is the most common malignancy of the human head and neck in the western hemisphere, and can originate in the glottic, supraglottic, or infraglottic regions.[27] The most common laryngeal tumors are located within the glottic region and are rarely associated with lymph node spread.[28,29] More than 90% of laryngopharyngeal carcinomas are of squamous cell origin.[21,30] Malignancies of the larynx generally arise from the surface epithelium and infiltrate deeper tissue.[30]

Detection of cartilage invasion is an important factor in the staging of laryngeal cancer. Direct diagnostic endoscopy is commonly used to view mucosal malignancies; however, deep extension of the tumors is most effectively assessed by CT and MRI. The inherently superior tissue contrast and resolution provided by MRI in differentiating among neoplasia, soft tissue, muscle, fat, and vessels has provided a distinct advantage over CT in evaluating human laryngeal pathology. Compared to CT, MRI has been shown to consistently produce superior soft tissue definition and resolution.[25] MR technology is reported to be the most effective means to diagnose and stage regional extension of laryngeal tumors and is useful in detecting cartilage invasion by neoplastic processes.[24,27,31,32] MRI has also been useful in the determination of the normal dimensions of the laryngeal framework of adult humans. These measurements have included the identification of the internal and external diameters of the cricoid cartilage, height and length of the thyroid cartilage in different planes, angle of the thyroid laminae, height of the arytenoid cartilages, width and length of the epiglottic cartilage, and internal and external diameter of first tracheal ring.[33] In 2002, a three-dimensional anatomic framework of the human larynx was created using MR technology.[34,35] This laryngeal model has proven useful in analysis of vocal fold opening and closing action during speech, swallowing, coughing, and voice production.[34] The MR recognition of the human laryngeal framework has also advanced the field of laryngeal electromyography and laryngeal surgery by providing a better understanding of the functional relationship of anatomical structures. The disadvantage of MRI for laryngeal imaging in human patients is that the technique is much more susceptible to motion artifacts that occur during swallowing, respiration, and from pulsatile flow of the great vessels in the neck.[23] Motion artifacts are reported to interfere with an accurate diagnosis in 10% to 15% of human

cases.[36] MRI also has a limited ability to detect histologic detail or microscopic spread of neoplastic cells.[30]

Optimum MR imaging protocols for the human larynx have been documented. T1-weighted spin echo MR images are typically the most helpful is defining normal laryngeal anatomy.[25,36] A 1.5 Tesla magnet and anterior neck surface coils are the current medical standard for laryngeal imaging.[23] T1-weighted spin echo axial (transverse) images are reported to be acquired using an intermediate 256 x 256 acquisition matrix. The use of a finer acquisition matrix of 512 x 512 was reported to produce improved visualization of anatomical detail, but scanning time was significantly increased.[36] A TR of 600 ms and a TE of 20 ms with a field of view of 20 cm for optimal T1-weighted imaging is reported in the current literature.[24] It is desirable to reduce the field of view as much as possible to improve spatial resolution. Slice thickness should be approximately 4mm for most MRI laryngeal applications.[31] Other reports exist that promote a slice thickness of 3 mm or 5mm with 1 mm between slice sections for optimum results.[23] Thinner slices have been reported to improve the visualization of anatomic detail, but require the completion of multiple acquisitions which are averaged, resulting in longer scanning times to maintain an equivalent signal to noise ratio.[36] A coronal T1-weighted imaging sequence should also be obtained using the same imaging parameters. A T1-weighted sagittal image is reported to be useful in determining the extent of neoplastic infiltration and is performed using the same imaging parameters.[37] A T2-weighted axial imaging sequence provides less spatial resolution, but has been shown to be useful in defining the interface between deep extension of the neoplasm and the surrounding normal soft tissue structures.[31] An in vitro study was conducted using a 2.35 Tesla MR imaging system and harvested human laryngeal specimens to compare the

effect of an increased magnetic field strength on acquired MR laryngeal images. A higher field strength using the 2.35 Tesla magnet produced T2-weighted images that were found to have superior resolution, improved tissue contrast, and better soft-tissue differentiation than the T1-weighted images produced.[38] When performed at a greater magnetic field strength, T2-weighted sequences are reported to have an improved potential to enable early detection of tumor invasion into the laryngeal cartilage.[38]

MR anatomy of the human larynx has been thoroughly reported in recent literature. MRI has been found very useful in delineating muscle planes, mucosal surfaces, and calcified laryngeal cartilage lamina. Noncalcified hyaline cartilage is reported to be of intermediate signal intensity and closely approximates the subcutaneous tissue and submucosal connective tissue.[25,31] The epiglottis is composed of fibroelastic cartilage and is of intermediate to high signal intensity.[25,31] High signal intensity was reported to be present along the surface of the laryngeal lumen due to the presence of the mucosal lining, which has a higher hydrogen concentration than the deeper cartilaginous structures.[24,37] A large proportion of the laryngeal skeleton of the adult human is composed of calcified cartilage and has a similar composition as cortical bone. The epiglottic cartilage consists of elastic cartilage and does not ossify, while the cricoid, thyroid, and arytenoid cartilages consist of hyaline cartilage, which demonstrates a predictable pattern of ossification with age.[39,40] Calcified laryngeal cartilage is reported to be of low signal intensity, with increased signal in the medullary space due to the presence of intra-medullary fat.[24,25,31,37] The thyroid cartilage has an inverted V configuration when viewed on an axial (transverse) MR image and has a characteristic trilaminar appearance.[24,41] The thyroid cartilage may appear irregular depending on the age of the patient and the pattern of calcification.[41] The cricoid

cartilage is readily identified and forms a broad posterior lamina, which is responsible for it's characteristic signet ring appearance.[24,41] The arytenoid cartilages are viewed as symmetrical areas of relatively high-signal intensity. The aryepiglottic folds have been reported to be well demonstrated on human laryngeal MRI sequences.[24] The aryepiglottic folds are largely composed of mucosal tissue covering a fatty infrastructure and are viewed as bright, high intensity signal. Generally, neoplasia is identified as having intermediate signal intensity on T1 – weighted sequences. On T2-weighted images, neoplasia usually has increased signal intensity compared with that found on T1-weighted images.[36] The preepiglottic space consists of a high abundance of fat and creates a bright signal. Disruption of this bright signal by an intermediate intensity signal has been reported to indicate tumor invasion.[24] Nonossified laryngeal cartilage also appears as intermediate signal intensity on T1-weighted images. Therefore, distinguishing neoplastic tissue from nonossified laryngeal cartilage presents a challenge.[23,24] Reports of false positive findings exist in the MRI diagnosis of cartilage invasion by neoplastic cells. The false positive findings resulted from the presence of inflammatory changes within tissue adjacent to the tumor, by fibrosis, or extramedullary hematopoiesis.[32,42] MRI is also limited in its ability to distinguish residual from recurrent laryngeal neoplasia.[30] Currently, laryngeal cancer is detected by an alteration and distortion in the appearance of normal tissue planes in representative T1-weighted images.[30] In one study of invasion of laryngeal cartilage by neoplasia, MRI had a specificity of 88% and a sensitivity of 89%, supporting MRI use in the evaluation of laryngeal cancer.[43] In radiologic-pathologic studies of laryngeal cartilage invasion, it has been demonstrated that MRI is more sensitive (89%) than CT imaging (64%) for the detection of tumoral infiltration of the laryngeal cartilages.[44,45]

The correlation between human MRI laryngeal anatomy and histologic specimens has been reported in several studies.[46,47] A study by Sakai and coworkers compared the normal MRI anatomy of the human larynx at a high field strength of 1.5 Tesla in 2 normal excised larynges and 62 subjects without laryngopharyngeal disease.[47] The larynges were sectioned transversely and the MR images were compared to gross and histologic sections. In the 62 subjects, MR at 1.5 T provided excellent anatomical detail of the major laryngeal cartilages, extrinsic and intrinsic laryngeal musculature, and soft tissues including the vocal cords, laryngeal ventricles, and aryepiglottic folds.[47] There was also a reported high correlation between the MR images and the corresponding gross histologic specimens. Unossified hyaline cartilage was found to be intermediate in signal intensity on T1-weighted and proton density images and low intensity on T2-weighted images. The signal intensity from ossified cartilage was determined by the amount of fatty marrow and was high in intensity on T1-weighted and proton density images and low to intermediate in intensity on T2-weighted images.[47] The epiglottic cartilage demonstrated an intermediate signal intensity on T1-weighted images and higher intensity on proton density and T2-weighted images. The intrinsic laryngeal muscles were well demonstrated as low intensity structures. In a study by Champsaur and coworkers, eight harvested laryngeal anatomic specimens were studied: four in the transverse plane, two in the sagittal plane, and two in the frontal plane.[46] The MRI and histologic sections were made at the same level through the larynx and were of similar slice thickness. Comparison showed all major anatomic laryngeal structures could be identified and excellent correlation existed between the MRI and histologic specimens.[46]

MRI OF THE LARYNX IN VETERINARY MEDICINE

Veterinary laryngeal MR imaging consists of a single report in normal dogs.[48] The goal of the study was to provide MRI reference images of the canine larynx in the sagittal and transverse planes, using a T1-weighted spin-echo sequence. The dogs were anesthetized and positioned into a horizontal bore Toshiba Vectra System with a superconducting magnet operating at a magnetic field strength of 0.5 Tesla using a human head radiofrequency coil. The sequence used was spin-echo type T1-weighted with a short pulse repetition time (TR) and a short echo time (TE). Sagittal series were obtained with a TR of 500 msec and TE of 25 msec. Transverse series were obtained with a TR of 450 msec and TE of 25 msec.[48]

The sagittal views revealed high signal in the epiglottis and corniculate processes of the arytenoid cartilages. The body of the arytenoid cartilage was intermediate in signal intensity. The lamina of the cricoid cartilage showed lower signal intensity than the epiglottis. The laryngeal musculature was intermediate in signal intensity and could be clearly differentiated from the cartilaginous structures. The thyroid cartilage was fount to be of low signal intensity due to the hyaline composition. Cavities filled with air, such as the airway lumen, pharynx, and nasal passages, corresponded to signal voids.[48]

The transverse MR images provided a more accurate anatomic representation of the laryngeal structures. In these sequences, all laryngeal cartilages could be differentiated. The lamina of the cricoid and thyroid cartilages were well defined and of low intensity signal. Adjacent to the lamina of the cricoid cartilage, the cricoarytenoideus dorsalis muscle was identified as intermediate signal intensity that enhanced the cricoid lamina morphology. The cartilaginous

structures of high signal intensity consisted of the epiglottis, corniculate process, and other areas of the arytenoid cartilages. The vocal folds were clearly defined on the transverse sequences.[48]

Overall, the study reported that the laryngeal cartilages had different signal intensities based on the tissue water content. The highest signal intensity was shown in the epiglottis and corniculate process of the arytenoid cartilages. The vocal folds were also present with a high intensity tissue signal. The MRI characteristics of these structures were thought to be due to their elastic nature. The cricoid and thyroid cartilages contained intermediate signal intensity due to their hyaline composition. The study speculated MRI technology to be of value in the diagnostic imaging of canine respiratory disease.[48]

EQUINE LARYNGEAL PATHOLOGY

The flexible fiberoptic endoscope has enhanced the examination of the equine larynx. In 1980, arytenoid chondritis in seven thoroughbred horses experiencing exercise intolerance and inspiratory dyspnea during exercise was described.[49] In 1988, 75 horses with arytenoid cartilage abnormalities were endoscopically compared and identified to have asymmetry of the rima glottidis and the inability to abduct the affected cartilage.[7]

Arytenoid chondritis is an infectious, usually progressive, disease in which the affected cartilage becomes thickened and distorted. A septic process gains access to the cartilage and results in inflammation and sinus tract formation with recurrent drainage.[50,51] Abscessation is common, but it is often detected only after it has become organized and has deformed the cartilage. This disease may be unilateral or bilateral with diagnosis established by endoscopic examination to

identify axial displacement and the abnormal appearance of a thickened arytenoid.[50] Palpation via a laryngotomy and radiography may also be used to detect arytenoid deformities. Radiographic changes of the larynx that occur in the condition of arytenoid chondritis include enlargement and increased density of the arytenoid cartilage with abnormal patterns of dystrophic mineralization or osseous metaplasia.[52,53] These radiographic findings must be interpreted with caution because it has also been reported that ossification of the laryngeal cartilages may occur naturally with age in the horse.[53] Radiographic abnormalities are not pathognomonic of laryngeal dysfunction.

The management of arytenoid chondritis consists of arytenoidectomy or debridement of infected arytenoid tissue. Severely thickened arytenoid cartilages must be removed.[3-6] Partial arytenoidectomy removes all of the arytenoid except the muscular process.[6] A 1988 study by Tulleners, et al., reported that 45% of thoroughbred racehorses and 20% of standardbred horses raced successfully after a partial arytenoidectomy.[7] Recent literature indicates a more optimistic success rate of 60%-80% return to racing is possible.[1,2]

Sullins reported an endoscopically guided minimally invasive laser-assisted debridement of infected cartilages that were not permanently deformed.[9] A stab incision is made in the cricothyroid membrane for insertion of a trocar to transmit a laser fiber and instruments to be guided endoscopically to debride the arytenoid lesion.[8,9] This procedure is performed in the standing horse with minimal post-operative healing time and has a very high success rate. Case selection is critical; the limitation of this technique is that it is effective only when arytenoid mobility can be regained. Acute swelling can subside, and abscesses can be drained, but it can

be difficult to determine whether moderately affected cartilages can be salvaged.[8,9] The use of MRI may help identify irreversible lesions.

FOOTNOTES

[a] Equiscan 3000, Hallmarq Veterinary Imaging Limited, Surrey, England.

[b] Magnetom Vision-Sonata horizontal long-bore, Siemens Medical Solutions Inc., Malvern, PA, 19355, USA.

REFERENCES CITED

1. Barnes AJ, Slone DE, Lynch TM. Performance after partial arytenoidectomy without mucosal closure in 27 Thoroughbred racehorses. *Vet Surg* 2004;33:398-403.

2. Parente EJ. Partial arytenoidectomy for treatment of failed laryngoplasty or arytenoid chondritis in racehorses., in *Proceedings*. 48th Annual Convention of the American Association of Equine Practitioners 2003;373-376.

3. Dean PW, Cohen ND. Arytenoidectomy for advanced unilateral chondropathy with accompanying lesions. *Vet Surg* 1990;19:364-370.

4. Tulleners EP, Harrison IW, Mann P, et al. Partial arytenoidectomy in the horse with and without mucosal closure. *Vet Surg* 1988;17:252-257.

5. Speirs VC. Partial arytenoidectomy in horses. *Vet Surg* 1986;15:316-320.

6. White NA, Blackwell RB. Partial arytenoidectomy in the horse. *Vet Surg* 1980;9:5-12.

7. Tulleners EP, Harrison IW, Raker CW. Management of arytenoid chondropathy and failed laryngoplasty in horses: 75 cases. *J Am Vet Med Assoc* 1988;192:670-675.

8. Sullins KE. Minimally invasive laser treatment of arytenoid chondritis in horses. *Clin Tech Eq Prac* 2002;1:13-16.

9. Sullins KE. Minimally invasive laser treatment of arytenoid chondritis in five horses. In: Proceedings 47th Annu Conv Am Assoc Equine Practnr 2001;120-122.

10. Bloch F, Hanson WW, Packard M. Nuclear induction. *Phys Rev* 1946;69:127.

11. Purcell EM, Torrey HC, Pound RV. Resonance absorption by nuclear magnetic moments in a solid. *Phys Rev* 1946;69:37-38.

12. Damadian R. Tumor detection by nuclear magnetic resonance. *Science* 1971;171:1151-1153.

13. Damadian R, Minkoff L, Goldsmith M, et al. Field focusing nuclear magnetic resonance: visualization of a tumor in a live animal. *Science* 1976;194:1430-1432.

14. Lauterbur P. Image formation by induced local interaction; examples employing magnetic resonance. *Nature* 1973;242:192.

15. Damadian R, Minkoff L, Goldsmith M. Whole-body nuclear magnetic resonance scanning: nmr studies of tumor cells. *Ciba Foundation Symposium* 1978;67:131-141.

16. Kaplan PA, Helms CA, Dussault R, et al. *Musculoskeletal MRI*. Philadelphia: W B Saunders, 2001: 1-23.

17. Haacke EM, Brown RW, Thompson MR, et al. *Magnetic Resonance Imaging: physical principles and sequence design*. New York, NY: John Wiley and Sons, Inc., 1999:1-62.

18. Westbrook C, Kaut C. *MRI in Practice*. Oxford: Blackwell Scientific, 1993:12-35.

19. Chan KK, Pathria M. MRI of the Musculoskeletal System In: Lufkin RB, Bradley WG,Zawadzki MB, eds. *Lippincott Williams & Wilkins MRI Teaching File Series*. Second Edition ed. Philadelphia: Lippincott Williams & Wilkins, 2001:1-205.

20. Stark DD, Bradley WG. *Magnetic Resonance Imaging*. Third Edition ed. New York, NY: C V Mosby, 1999:9-520.

21. Stark DD, Moss AA, Gamsu G. Magnetic resonance imaging of the neck: Part 2. Pathologic findings. *Radiology* 1983;150:455-461.

22. Dyce KM, Sack WO, Wensing CJG. *Textbook of Veterinary Anatomy*. 2nd Edition ed. Philadelphia: WB Saunders Company, 1996:155-160.

23. Curtin HD. Imaging of the larynx: current concepts. *Radiol* 1989;173:1-11.

24. Towler CR, Young SW. Magnetic resonance imaging of the larynx. *Magn Reson Q* 1989;5:228-241.

25. Teresi LM, Lufkin RB, Hanafee WN. Magnetic resonance imaging of the larynx. *Radiol Clin North Am* 1989;27:393-406.

26. Shorten GD, Opie NJ, Graziotti P, et al. Assessment of upper airway anatomy in awake, sedated and anaesthetised patients using magnetic resonance imaging. *Anaesth Intensive Care* 1994;22:165-169.

27. Castelijns JA, Kaiser MC, Valk J, et al. MR imaging of laryngeal cancer. *J Comput Assist Tomogr* 1987;11:134-140.

28. Kirchner JA. Two hundred laryngeal cancers: Patterns of growth and spread as seen in serial section. *Laryngoscope* 1987;87:474-482.

29. Schneider M, Probst R, Wey W. Magnetic resonance imaging--a useful tool for airway assessment. *Acta Anaesthesiol Scand* 1989;33:429-431.

30. Hasso AN, Tang T. Magnetic resonance imaging of the pharynx and larynx. *Top Magn Reson Imaging* 1994;6:224-240.

31. Jabour BA, Lufkin RB, Hanafee WN. Magnetic resonance imaging of the larynx. *Top Magn Reson Imaging* 1990;2:60-68.

32. Atula T, Markkola A, Leivo I, et al. Cartilage invasion of laryngeal cancer detected by magnetic resonance imaging. *Eur Arch Otorhinolaryngol* 2001;258:272-275.

33. Eckel HE, Sittel C, Zorowka P, et al. Dimensions of the laryngeal framework in adults. *Surg Radiol Anat* 1994;16:31-36.

34. Selbie WS, Gewalt SL, Ludlow CL. Developing an anatomical model of the human laryngeal cartilages from magnetic resonance imaging. *J Acoust Soc Am* 2002;112:1077-1090.

35. Rubin JS, Summers P, Harris T. Visualization of the human larynx: a three-dimensional computer modeling tool. *Auris Nasus Larynx* 1998;25:303-308.

36. Castelijns JA, van den Brekel MW, Hermans R. Imaging of the larynx. *Semin Roentgenol* 2000;35:31-41.

37. Stiglbauer R, Steurer M, Schimmerl S, et al. MRI of cartilaginous tumors of the larynx. *Clin Radiol* 1992;46:23-27.

38. Kikinis R, Wolfensberger M, Boesch C, et al. Larynx: MR imaging at 2.35 T. *Radiology* 1989;171:165-169.

39. Fatterpekar GM, Mukherji SK, Rajgopalan P, et al. Normal age-related signal change in the laryngeal cartilages. *Neuroradio* 2004;46:678-681.

40. Claassen H, Kirsch T, Simons G. Cartilage canals in human thyroid cartilage characterized by immunolocalization of collagen types I, II, pro III, IV, and X. *Anat Histol Embryol* 1996;94:147-153.

41. Branstetter BFt, Weissman JL. Normal anatomy of the neck with CT and MR imaging correlation. *Radiol Clin North Am* 2000;38:925-940, ix.

42. Becker M, Zbaren P, Laeng H, et al. Neoplastic invasion of the laryngeal cartilage: comparison of MR imaging and CT with histopathologic correlation. *Radiology* 1995;194:661-669.

43. Castelijns JA, Gerritsen GJ, Kaiser MC. MRI of normal and cancerous laryngeal cartilages: histologic correlation. *Laryngoscope* 1987;97:1085-1093.

44. Zbaren P, Becker M, Lang H. Pretherapeutic staging of laryngeal carcinoma. Clinical findings, computed tomography and magnetic resonance imaging compared with histopathology. *Cancer* 1996;77:1263-1273.

45. Yousem DM, Tufano RP. Laryngeal imaging. *Magn Reson Imaging Clin N Am* 2002;10:451-465.

46. Champsaur P, Parlier-Cuau C, Brunet C, et al. Serial anatomy of the larynx in MRI: MRI-histologic correlations. *Surg Radiol Anat* 2000;22:5-11.

47. Sakai F, Gamsu G, Dillon WP, et al. MR imaging of the larynx at 1.5 T. *J Comput Assist Tomogr* 1990;14:60-71.

48. Vazquez JM, Arencibia A, Gil F, et al. Magnetic resonance imaging of the normal canine larynx. *Anat Histol Embryol* 1998;27:263-270.

49. Haynes PF, Snider TG, McClure JR, et al. Chronic chondritis of the equine arytenoid cartilage. *J Am Vet Med Assoc* 1980;177:1135-1142.

50. Haynes PF. Arytenoid chondritis in the horse. *In: Proceedings 27th Annu Conv Am Assoc Equine Practnr* 1981;27:63-69.

51. McKillop KL. Experimental induction of arytenoid chondritis in the horse. Masters Thesis. Davis, CA: University of California, 1982.

52. Orsini PG, Raker CW, Reid CF, et al. Xeroradiographic evaluation of the equine larynx. *Am J Vet Res* 1989;50:845-849.

53. Shapiro J, White NA, Schlafer DH, et al. Hypertrophic ossification of the laryngeal cartilages of a horse. *J Equine Med Surg* 1979;3:370-374.

Magnetic Resonance Imaging of the Normal Equine Larynx

Cortney E. Henderson* DVM

Kenneth E. Sullins* DVM, MS, DACVS

C. Douglas Philips° MD FACR

From the Marion duPont Scott Equine Medical Center*

Virginia-Maryland Regional College of Veterinary Medicine

PO Box 1938

Leesburg, Virginia 20177

and the Department of Radiology°

University of Virginia

PO Box 800170

Charlottesville, Virginia 22908

Funded by the Patricia Bonsall Stuart Equine Research Award.

Submitted to: American Journal of Veterinary Research

Abstract

Objective: To establish the appearance of normal equine laryngeal cartilages as detected by magnetic resonance imaging.

Animals: Specimens were acquired from clinically normal horses that were euthanized for reasons other than respiratory disease.

Procedure: Three *in situ* and 5 *ex vivo* larynges were imaged using a 0.3 Tesla system. Images were obtained in the transverse plane using T1-weighted 3D spin echo, T2-weighted 3D spin echo, T2-weighted gradient echo, short tau inversion recovery (STIR), and proton density spin echo sequences. Five *ex vivo* larynges were also imaged in the transverse plane using the 1.5 Tesla sequences including T1-weighted 3D spin echo, T2-weighted 3D turbo-spin echo, turbo inversion recovery (TIRM), and proton density spin echo sequences. A frozen gross laryngeal specimen was sliced in 5-mm transverse sections for comparison to the MR images.

Results: A high correlation was found between MR images and the gross transverse sections. Successful imaging was accomplished using both imaging systems; however, the 1.5 Tesla system yielded superior image resolution. The 0.3 Tesla imaging system could accommodate the intact equine head, which was not possible using the 1.5 Tesla MRI system. The internal morphology of the laryngeal cartilages was clearly identified on all imaging sequences obtained. Cartilages were found to differ in signal intensity based on the tissue composition and imaging sequences performed.

Conclusion: MRI was determined to be a useful imaging modality for evaluating the cartilage morphology of the equine larynx.

Introduction

Disease of the equine larynx limits performance by causing exercise intolerance and abnormal upper respiratory noise. Traditional evaluation of the equine larynx is based on physical examination, upper airway endoscopy, and radiography. While these diagnostic tools are used to diagnose certain laryngeal disorders, the majority of the structure of the laryngeal cartilages cannot be thoroughly evaluated.

Arytenoid chondritis is an acute or chronic, often progressive bacterial infection that results in thickening of the arytenoid cartilage and airway obstruction. Affected horses experience exercise intolerance and abnormal respiratory noise and complete airway obstruction is possible in advanced disease states or during strenuous exercise. Traditional treatment has been partial arytenoidectomy with the horse under general anesthesia.[1-6] Although racing is possible following arytenoidectomy, the procedure has potential complications and is costly.[1,2,7] An alternative minimally invasive procedure consisting of laser-assisted debridement has been reported in the standing horse if the condition is recognized before permanent arytenoid deformity has occurred.[8,9] Case selection is critical; the diagnostic challenge lies in determining the extent of arytenoid deformity in marginal cases. Endoscopy, radiology, and ultrasound have not fulfilled this need. Magnetic resonance imaging (MRI) has previously has led to advances in equine orthopedics and its application to the equine larynx would prove useful. MRI of the equine larynx would improve current diagnostic ability, limit invasive treatment techniques, and aid in the decision to debride or remove an affected arytenoid cartilage.

Magnetic resonance imaging provides a detailed depiction of the morphology and composition of the tissue based on hydrogen content.[10] Images are produced in gray scale with specific intensities of signal based on the tissue composition. Normal MRI characteristics of the larynx have been reported in human and veterinary medicine. MRI has been found very useful in delineating muscle planes, mucosal surfaces, and calcified laryngeal cartilage lamina. In humans and canines, noncalcified laryngeal hyaline cartilage is reported to be of intermediate signal intensity.[11-13] The epiglottis is composed of fibroelastic cartilage and is of intermediate to high signal intensity.[11-13] High signal intensity is reported to be present along the surface of the laryngeal lumen due to the presence of the mucosal lining, which has a higher hydrogen concentration than the deeper cartilaginous structures.[13-15] Calcified laryngeal cartilage, such as is found in the thyroid, cricoid, and arytenoid cartilages, is reported to be of low signal intensity, with increased signal within the medullary space due to the presence of fat.[11-15] The aryepiglottic folds are largely composed of mucosal tissue covering a fatty infrastructure and are viewed as high intensity signal.[14]

Previous reports of MRI of the equine larynx do not currently exist. The magnet configuration and field strength are limited in equine veterinary medicine to equipment that is available in a clinical setting. The purpose of the study reported here was to acquire clinically useful MR images of the normal equine larynx using the 0.3 Tesla permanent open magnet MRI system that is currently available in clinical practice. Images were also obtained using a 1.5 Tesla superconducting horizontal magnet for comparison. The images acquired were compared with similar slices of a gross anatomic specimen. The intent of this study was to evaluate MRI imaging of the normal equine larynx, so the severity of internal laryngeal cartilage lesions could

be determined in clinical cases. We hypothesized that MRI would offer a useful, noninvasive means for evaluation of the morphology of the equine laryngeal cartilages and that the images obtained would correlate well with gross anatomic specimens. An objective of the study was to devise a diagnostic standard for normal magnetic resonance imaging to provide a comparison for laryngeal disease.

Materials and methods

Specimens were obtained from hospital cases that were euthanized for reasons unrelated to respiratory disease. Specimens were harvested promptly after euthanasia and verified to have grossly normal laryngeal anatomy. Heads were harvested at the mid-cervical area and frozen at -20°C until thawed for imaging. *Ex vivo* larynges including extrinsic musculature and proximal trachea were harvested. Larynges were also frozen at -20°C until thawed for imaging. Three *in situ* larynges and 5 *ex vivo* larynges were imaged using a 0.3 Tesla MRI system[a] and 5 *ex vivo* larynges were imaged using a 1.5 Tesla MRI system[b].

The 0.3 Tesla system[a] consisted of a permanent open magnet (C-shaped) operating at a magnetic field strength of 0.3 Tesla. For the *in situ* specimens, a circular-polarized, transmit and receive equine hoof radio-frequency coil[c] was positioned on the ventral aspect of the throat and centered over the larynx. A flexible, saddle configuration radio-frequency surface coil was also developed for use in the study to reduce the signal-to-noise ratio and improve image resolution. The saddle coil was contoured to the ventral aspect of the throat and encompassed the lateral and ventral sides of the larynx. Each head was positioned so that the larynx was within the isocenter of the magnet. The long axis of the neck was placed perpendicular to the long axis of the magnet to mimic the clinical scenario for anesthetized horses. Images were acquired in the transverse plane using an image acquisition matrix of 256 x 256 pixels with a field of view of 16.9 cm. Sequences performed consisted of T1-weighted 3D spin echo, T2-weighted 3D spin echo, T2-weighted gradient echo, proton density spin echo, and short tau inversion recovery (STIR). The T1-weighted 3D spin echo pulse sequence had a short pulse repetition time (TR) of 23 ms and

short echo time (TE) of 7 ms with a slice thickness of 4 mm. The T2-weighted 3D spin echo pulse sequence had a long TR of 1800 ms and a short TE of 30 ms with a slice thickness of 4 mm. T2-weighted gradient echo pulse sequence had a short pulse repetition time TR of 34 ms and short echo time TE of 13 ms with a slice thickness of 4 mm. The proton density spin echo pulse sequence had a long TR of 1100 ms and a short TE of 24 ms with a slice thickness of 3 mm. The short tau inversion recovery STIR sequence had a long TR of 1800 ms and a short TE of 28 ms with a 5 mm slice thickness.

Five *ex vivo* larynges were also imaged with the 0.3 Tesla magnet[a]. Each specimen was placed in the center of a circular-polarized, transmit and receive equine hoof radio-frequency coil[c] and positioned so that the larynx was within the isocenter of the magnet. The images were acquired in the transverse plane, but sagittal images were acquired for referencing. The image acquisition matrix for all transverse series was 256 x 256 pixels. T1 and T2 sequences had a field of view of 17 cm and slice thickness of 4 mm with 24 slices made in a transverse plane. The proton density and inversion recovery series had a slightly larger field of view of 19.2 cm with slice thickness of 3 mm and 5 mm respectively, with 8 slices made in the transverse plane through each specimen. Sequences performed consisted of T1-weighted 3D spin echo, T2-weighted 3D spin echo, T2-weighted gradient echo, proton density spin echo, and short tau inversion recovery STIR. The T1-weighted 3D spin echo pulse sequence used had a short pulse repetition time TR of 23 ms and short echo time TE of 7 ms. The T2-weighted 3D spin echo pulse sequence used had a long TR of 1800 ms and a short TE of 30 ms. T2-weighted gradient echo pulse sequence had a short pulse repetition time TR of 34 ms and short echo time TE of 13 ms. The proton density spin

echo pulse sequence used had a long TR of 1000 ms and a short TE of 25 ms. The short tau inversion recovery STIR sequence had a long TR of 1800 ms and a short TE of 28 ms.

Five *ex vivo* larynges were also imaged using a superconducting magnet[b], operating at a magnetic field strength of 1.5 Tesla. Each larynx was placed longitudinally into a circular-polarized, transmit and receive radio-frequency extremity coil[d] and the images were acquired in the transverse plane; sagittal images were acquired for referencing the position of the transverse sections. The image acquisition matrix for the T1 and T2 transverse series was 259 x 320 pixels with a field of view of 18 cm. This configuration generated voxel sizes of .6 x .6 x 4 mm. The proton density and inversion recovery series had a slightly larger voxel size of .9 x .7 x 4 mm and .7 x .7 x 4 mm respectively. Slice thickness was standardized at 4 mm for all specimens and 21 slices were made in a transverse plane through each specimen. Sequences performed consisted of T1-weighted 3D spin echo, T2-weighted 3D turbo-spin echo, proton density spin echo, and a turbo inversion recovery (TIRM) with a slice selective inversion pulse of 150ms. The T1-weighted 3D spin echo pulse sequence used had a short pulse repetition time TR of 519 ms and short echo time TE of 15 ms. The T2-weighted turbo-spin echo pulse sequence used had a long TR of 5000 ms and a long TE of 109 ms. The proton density spin echo pulse sequence used had a long TR of 2000 ms and a short TE of 20 ms. The inversion recovery sequence TIRM had a long TR of 4680 ms and a short TE of 24 ms.

Results

0.3 Tesla system and *in situ* larynges

The 0.3 Tesla imaging system[a] was found to produce an accurate anatomic depiction of the equine larynx *in situ*, using the T1-weighted 3D spin echo, T2-weighted 3D spin echo, T2-weighted gradient echo, proton density spin echo, and short tau inversion recovery STIR sequences. The width of the open permanent magnet was limited to 23 cm, which restricted the size of equine head to be imaged. The equine hoof radio-frequency coil functioned adequately as a surface coil when applied to the ventral aspect of the throat. The flexible, saddle configuration radio-frequency surface coil proved to be nonfunctional due to failure of calibration with the 0.3 Tesla imaging system. Acquired images from the 0.3 Tesla imaging system[a] accurately identified most laryngeal structures; however, image resolution substantially decreased as tissue depth increased. The T1-weighted 3D spin echo sequence subjectively produced the highest image resolution and structural definition. T1-weighted 3D spin echo sequences were also the least susceptible to loss of image resolution due to increased tissue depth. Despite lower image resolution, the *in situ* MR images correlated well with signal intensity characteristics of the *ex vivo* larynges in both systems.

0.3 Tesla system and *ex vivo* larynges

The 0.3 Tesla imaging system[a] produced image quality, resolution, and tissue contrast that was superior in the *ex vivo* larynges compared to the *in situ* specimens based on subjective evaluation. The equine hoof radio-frequency coil accommodated the *ex vivo* larynx well and tissue depth did not affect image resolution. The laryngeal structures viewed with the T1-

weighted 3D spin echo, T2-weighted 3D spin echo, T2-weighted gradient echo, proton density spin echo, and short tau inversion recovery STIR sequences were found to have consistent MR signal intensity characteristics of each structure imaged. The signal characteristics correlated well with images produced from the 1.5 Tesla system[b]. Anatomic structures were accurately depicted and cartilage morphology was easily evaluated. T1-weighted 3D spin echo imaging subjectively produced greater resolution and definition of normal laryngeal structures, but was found to lack image contrast compared to the T2-weighted and inversion recovery sequences. T2-weighted 3D spin echo and inversion recovery sequences were very similar in appearance and provided the highest image contrast. Proton density sequences yielded similar tissue resolution when compared to the T1-weighted sequences, but had the least tissue contrast of the sequences evaluated. All acquired 0.3 Tesla images proved to have excellent correlation with gross anatomic specimens.

1.5 Tesla system and *ex vivo* larynges

The 1.5 Tesla system[b] was found to produce high anatomic resolution of the *ex vivo* equine larynges; however, the machine could not accommodate the entire equine head for *in vivo* MRI. Acquired images accurately and clearly identified the individual laryngeal structures on all imaging sequences and produced consistent MR signal characteristics of the specific structure. The image quality, resolution, and tissue contrast were found to be superior to the *in situ* and *ex vivo* larynges of the 0.3 Tesla system based on subjective comparison of the acquired images. Differentiation of normal anatomic structures and image resolution was superior with T1-weighted 3D spin echo imaging sequences. Contrast between the laryngeal cartilages and the surrounding soft tissue was enhanced by the T2-weighted, inversion recovery, and proton density

sequences when subjectively compared to the T1 weighted sequences. T2-weighted turbo-spin echo and turbo inversion recovery (TIRM) sequences were found to be very similar in signal characteristics. Proton density spin echo sequences were found to be the least desirable images evaluated and had lower anatomic resolution and decreased tissue contrast. All acquired 1.5 Tesla MR images proved to have excellent correlation with gross anatomic specimens.

MRI signal characteristics of laryngeal structures

The equine larynges were well evaluated with both imaging systems. The mucosa was a thin margin of high signal intensity enclosing the perimeter of the airway lumen and was similar in all imaging sequences. The cricoid cartilage lamina was clearly defined as a continuous ring of intermediate to low signal intensity, surrounding the caudal laryngeal lumen (Figure 1). The dorsal spine of the cricoid cartilage provided a reference point. The cricoid cartilage lamina on T2-weighted, proton density, and inversion recovery sequences contained low signal compared to the T1-weighted sequences (Figure 2, 3). The MRI representation of the cricoid cartilage correlated well with the gross anatomic sectioned specimen (Figure 4).

The arytenoid cartilages were well defined structures of varying signal intensity. The outer composition of the arytenoid bodies had a homogenous, intermediate signal on the T1 weighted images (Figure 5, 6). In the center of the arytenoid cartilages, a core increased signal intensity represented a small medullary cavity (Figure 5). The cricoarytenoideus lateralis and thyroarytenoideus muscles were homogenous structures of intermediate signal on the T1-weighted images had increased signal intensity on the T2- weighted and inversion recovery sequences (Figure 5, 6, 7). The dorsal region of the arytenoid cartilages lacked resolution on the

in situ specimens (Figure 8). The MRI representations of the arytenoid cartilages correlated well with the gross anatomic specimen (Figure 9). The linear thyroid cartilage lamina was a low signal structure on all imaging sequences. It also produced bright signal intensity of fat within a small medullary cavity most evident on the T2-weighted and inversion recovery sequences (Figure 10, 11). The MR images of the thyroid cartilages correlated well with the gross specimens (Figure 12).

The vocal folds were represented as well defined linear structures with increased signal intensity on all imaging sequences. The laryngeal ventricles were very pronounced foci of signal void with a high signal mucosal lining (Figure 10, 11, 13). The laryngeal ventricles were imaged in the *in situ* specimens; however, tissue resolution was poor (Figure 14). The corniculate processes of the arytenoid cartilages were elongated structures of variable signal intensity, but contained higher signal intensity than the arytenoid body and muscular process on all imaging sequences (Figure 15, 16, 17). Excellent correlation was produced between the MR images of the corniculate processes and the gross specimens (Figure 18).

Discussion

MRI was a useful modality for the evaluation of the internal morphology of the equine laryngeal cartilages *in situ* and *ex vivo*. The 0.3 Tesla imaging system[a] was chosen due to its current availability in equine clinical practice. The aim of this study was to produce laryngeal MR images that could be duplicated with anesthetized horses in a clinical setting. This goal was accomplished with the 0.3 Tesla system and *in situ* larynges. The *in situ* laryngeal specimens provided an accurate model that can be applied for imaging of the anesthetized patient. The open magnet of the 0.3 Tesla MRI system accommodated an equine head of 23 cm or less in width, which is similar to the dimensions of a racing Thoroughbred. The *in situ* and *ex vivo* laryngeal specimens were frozen and thawed once prior to imaging. The effect of freezing and thaw on tissue MRI characteristics and the resulting images was not known and may have effected the results of the study. Different laryngeal specimens were used in each imaging phase of the study, which minimized the tissue effect of repetitive freezing and thaw.

Limitations of the 0.3 Tesla imaging system and *in situ* larynges occurred due to decreased image resolution as distance from the coil increased since it was not possible to position the *in situ* specimen and the radio-frequency coil into the isocenter of the magnet simultaneously. This limitation proved detrimental to image quality and would likely be improved with an alternative coil configuration. One such alternative has been reported in human literature and consists of a solenoidal surface coil wrapped around the neck.[11,16] The solenoidal surface coil is commonly implemented in human laryngeal MRI and fulfills the imaging criteria that the axis of the surface coil must be orthogonal to the axis of the main magnetic field.[11,17] The solenoidal configuration

is reported to significantly improve the signal-to-noise ratio over standard human head and neck coils by 45% - 48%.[11] A second radio-frequency surface coil that is reported to significantly decrease the signal-noise ratio is the saddle configuration.[11] The saddle coil encompasses the larynx on the lateral and ventral sides and when positioned within the isocenter of the magnet, image production is reported to be superior compared to standard coil configurations. In preparation for the study reported here, a saddle configuration radio-frequency coil was developed. The coil proved to be ineffective and non-functional due to coil positioning issues and difficulty in calibration with the 0.3 Tesla system. Therefore, the developed saddle configuration coil was excluded from the results of the present study.

Internal morphology of the equine *ex vivo* larynges were evaluated with the 0.3 Tesla and the 1.5 Tesla imaging systems. As mentioned previously, the 0.3 Tesla system is readily available to the equine clinician in veterinary practice; therefore, an need to define normal MRI laryngeal anatomy for that system exists. The 1.5 Tesla imaging system was included in the study for comparison because the system is the current medical standard for human laryngeal imaging.[18] The 1.5 Tesla system would not accommodate equine larynges *in situ*, was a disadvantage compared to the 0.3 Tesla system. The equine hoof radio-frequency coil[c] and the circular-polarized, transmit and receive radio-frequency extremity coil[d], were both found to accommodate the *ex vivo* laryngeal specimens. Both systems produced clear, diagnostic quality images; however, tissue resolution, contrast, and detail were improved with the 1.5 Tesla system. The study reported here was consistent with human literature that reports improvement in image quality with increasing magnetic field strength. An *ex vivo*, human study was conducted using a 2.35 Tesla MR imaging system and *ex vivo* laryngeal specimens to compare the effect of

increased magnetic field strength on laryngeal images. A higher field strength using the 2.35 Tesla magnet produced T2-weighted images with superior resolution and improved tissue contrast than the T1-weighted images.[19] The findings of the present study are consistent with those reported by Kikinis et al. in that the T2-weighted imaging sequences acquired with the 1.5 Tesla system were found to have the highest level of image contrast when compared to the T1-weighted images and to all of 0.3 Tesla system acquired images.

Optimum MR imaging protocols for the human larynges have been documented. An intermediate 256 x 256 acquisition matrix is preferred in human medicine for imaging the laryngeal structures; therefore, the same acquisition matrix was chosen for the study reported here.[20] T1-weighted 3D spin echo MR images are reported to be the most helpful in defining normal human laryngeal anatomy.[11,20] The study reported here correlated with previous reports in that T1-weighted images had superior tissue resolution and structural definition. However, image contrast was better expressed subjectively with T2-weighted and inversion recovery techniques. Previous reports considered it desirable to reduce the field of view as much as possible to improve spatial resolution.[14] This principle was applied in the current study by limiting the field of view to 16 – 18 cm. Slice thickness is reported to be approximately 4 mm for most MRI laryngeal applications.[12] Other reports exist that promote a slice thickness of 3 – 5 mm for optimum results.[18,20] The study reported here adhered to this recommendation and consisted of a limited slice thickness range of 3 mm – 5 mm. T2-weighted transverse imaging sequences are reported to provide less spatial resolution, but have been shown to be useful in defining the interface between deep extension of neoplasia and the surrounding normal soft tissue structures.[12] In the current study, the T2-weighted images had improved contrast when

subjectively compared to the other imaging sequences, a characteristic that may be helpful in localizing laryngeal pathology.

The *in situ* and *ex vivo* equine larynges were found to have consistent MRI signal intensity characteristics between imaging systems. Individual cartilage types were found to have consistent MRI characteristics when imaged with each sequence. Hyaline cartilage and fibroelastic cartilage compose the larynges of the horse and vary in degree of ossification.[21,22] Hyaline cartilage has low hydrophilic capacity and low hydrogen proton density and therefore, has a relatively low MR signal intensity.[13] Fibroelastic cartilage has a substantial hydrogen proton content and relatively high MR signal intensity.[13] Noncalcified hyaline cartilage is reported to be of intermediate signal intensity and closely approximates the subcutaneous tissue and submucosal connective tissue.[11-13] The results of the study reported here are consistent with these previously reported findings.

The cricoid, thyroid, and majority of the arytenoid cartilages have been shown to undergo variable age related ossification and are composed of hyaline cartilage.[21-25] Calcified laryngeal cartilage is reported to be of low signal intensity, with increased signal within the medullary space due to the presence of intra-medullary fat.[11,12,14,15] The characteristic of increased signal within the medullary space of the thyroid and arytenoid cartilages were observed in the present study. The thyroid cartilage had an inverted V configuration when viewed on transverse MR images and, as reported previously in the human and veterinary literature, was characterized by a trilaminar appearance.[13,14,26] The thyroid cartilage appeared irregular depending on the age of the patient and the pattern of calcification as reported in previous studies.[26]

The epiglottis and corniculate process of the arytenoid cartilages are composed of fibroelastic cartilage and are reported to be of high signal intensity.[11,12] Bright signal intensity was reported to be present along the surface of the laryngeal lumen due to the presence of the mucosal lining, which has a higher hydrogen concentration than the deeper cartilaginous structures.[13-15] This finding was also verified in the study reported here.

The correlation between human MRI laryngeal anatomy and anatomic specimens has been reported in several studies.[24,27] A study by Sakai and coworkers compared the normal MRI anatomy of the human larynx at a high field strength of 1.5 Tesla in 2 normal excised larynges and 62 subjects without laryngopharyngeal disease[24]. The transversely sectioned laryngeal specimens had excellent correlation to the acquired MR images. In a study by Champsaur and coworkers, eight harvested laryngeal anatomic specimens were studied with histological sections made at the same level through the larynx and were of similar slice thickness[27]. When compared to the histologic sections of this region, it was determined that all major anatomic laryngeal structures could be identified and there was excellent correlation between the two modalities. The results of this study support earlier reports in the human literature and found an excellent correlation of the MR images of *ex vivo* larynges with anatomic specimens.

In summary, MRI was determined to be an effective, noninvasive means of evaluation of the internal morphology of the equine larynges. The MRI characteristics of specific equine laryngeal structures were consistent with previous reports in the human and veterinary literature and correlated well with gross anatomic specimens. The technique will be useful in the clinical

setting in determining extent and severity of equine laryngeal pathology in such conditions as arytenoid chondritis.

Footnotes

[a] Equiscan 3000, Hallmarq Veterinary Imaging Limited, Surrey, England.

[b] Magnetom Vision-Sonata horizontal long-bore, Siemens Medical Solutions Inc., Malvern, PA, 19355, USA.

[c] Equine hoof radio-frequency coil, Hallmarq Veterinary Imaging Limited, Surrey, England.

[d]Circular-polarized, transmit and receive radio-frequency extremity coil, Siemens Medical Solutions Inc., Malvern, PA, 19355, USA.

References

1. Barnes AJ, Slone DE, Lynch TM. Performance after partial arytenoidectomy without mucosal closure in 27 Thoroughbred racehorces. *Vet Surg* 2004;33:398-403.

2. Parente EJ. Partial arytenoidectomy for treatment of failed laryngoplasty or arytenoid chondritis in racehorses., in *Proceedings.* 48th Annual Convention of the American Association of Equine Practitioners 2003;373-376.

3. Dean PW, Cohen ND. Arytenoidectomy for advanced unilateral chondropathy with accompanying lesions. *Veterinary Surgery* 1990;19:364-370.

4. Tulleners EP, Harrison IW, Mann P, et al. Partial arytenoidectomy in the horse with and without mucosal closure. *Veterinary Surgery* 1988;17:252-257.

5. Speirs VC. Partial arytenoidectomy in horses. . *Veterinary Surgery* 1986;15:316-320.

6. White NA, Blackwell RB. Partial arytenoidectomy in the horse. *Veterinary Surgery* 1980;9:5-12.

7. Tulleners EP, Harrison IW, Raker CW. Management of arytenoid chondropathy and failed laryngoplasty in horses: 75 cases. *J Am Vet Med Assoc* 1988;192:670-675.

8. Sullins KE. Minimally invasive laser treatment of arytenoid chondritis in horses. *Clin Tech Eq Prac* 2002;1:13-16.

9. Sullins KE. Minimally invasive laser treatment of arytenoid chondritis in five horses. In: Proceedings 47th Annu Conv Am Assoc Equine Practnr 2001;120-122.

10. Haacke EM, Brown RW, Thompson MR, et al. *Magnetic Resonance Imaging: physical principles and sequence design*. New York, NY: John Wiley and Sons, Inc., 1999.

11. Teresi LM, Lufkin RB, Hanafee WN. Magnetic resonance imaging of the larynx. *Radiol Clin North Am* 1989;27:393-406.

12. Jabour BA, Lufkin RB, Hanafee WN. Magnetic resonance imaging of the larynx. *Top Magn Reson Imaging* 1990;2:60-68.

13. Vazquez JM, Arencibia A, Gil F, et al. Magnetic resonance imaging of the normal canine larynx. *Anat Histol Embryol* 1998;27:263-270.

14. Towler CR, Young SW. Magnetic resonance imaging of the larynx. *Magn Reson Q* 1989;5:228-241.

15. Stiglbauer R, Steurer M, Schimmerl S, et al. MRI of cartilaginous tumours of the larynx. *Clin Radiol* 1992;46:23-27.

16. Lufkin RB, Votruba J, Reicher M. Solenoid surface coils in magnetic resonance imaging. *AJR* 1986;146:409-412.

17. Axel L. Surface coil magnetic resonance imaging. *J Comput Assist Tomogr* 1984;8:381.

18. Curtin HD. Imaging of the larynx: current concepts. *Radiology* 1989;173:1-11.

19. Kikinis R, Wolfensberger M, Boesch C, et al. Larynx: MR imaging at 2.35 T. *Radiology* 1989;171:165-169.

20. Castelijns JA, van den Brekel MW, Hermans R. Imaging of the larynx. *Semin Roentgenol* 2000;35:31-41.

21. Shapiro J, White NA, Schlafer DH, et al. Hypertrophic ossification of the laryngeal cartilages of a horse. *J Equine Med Surg* 1979;3:370-374.

22. Orsini PG, Raker CW, Reid CF, et al. Xeroradiographic evaluation of the equine larynx. *Am J Vet Res* 1989;50:845-849.

23. Fatterpekar GM, Mukherji SK, Rajgopalan P, et al. Normal age-related signal change in the laryngeal cartilages. *Neuroradiology* 2004;46:678-681.

24. Sakai F, Gamsu G, Dillon WP, et al. MR imaging of the larynx at 1.5 T. *J Comput Assist Tomogr* 1990;14:60-71.

25. Claassen H, Kirsch T, Simons G. Cartilage canals in human thyroid cartilage characterized by immunolocalization of collagen types I, II, pro III, IV, and X. *Anat Histol Embryol* 1996;94:147-153.

26. Branstetter BFt, Weissman JL. Normal anatomy of the neck with CT and MR imaging correlation. *Radiol Clin North Am* 2000;38:925-940, ix.

27. Champsaur P, Parlier-Cuau C, Brunet C, et al. Serial anatomy of the larynx in MRI: MRI-histologic correlations. *Surg Radiol Anat* 2000;22:5-11.

LIST OF FIGURES

Page

FIGURES

Figure 1: *ex vivo*

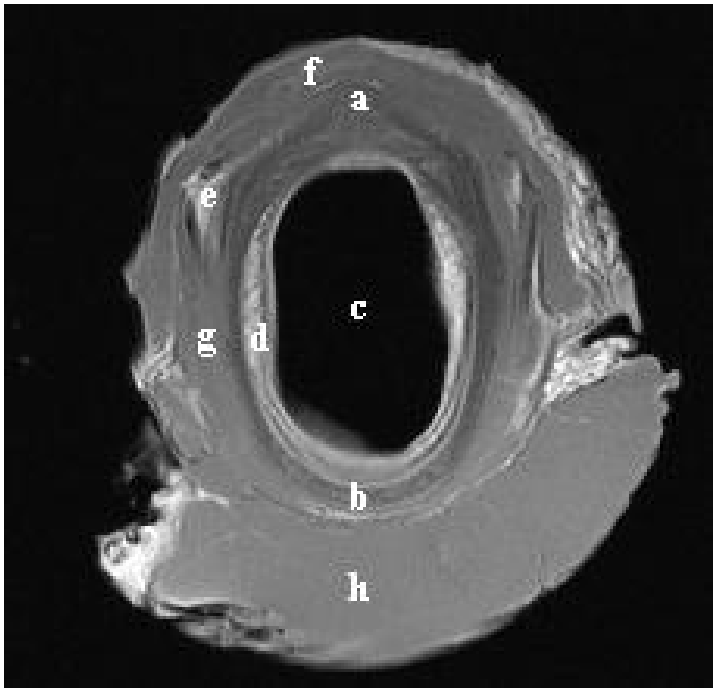

Figure 2: *ex vivo*

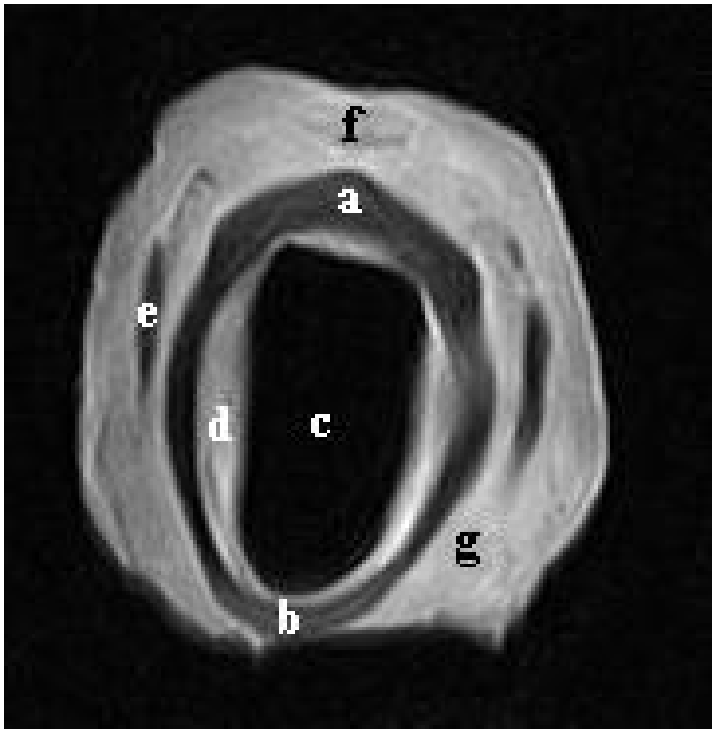

Figure 3: *ex vivo*

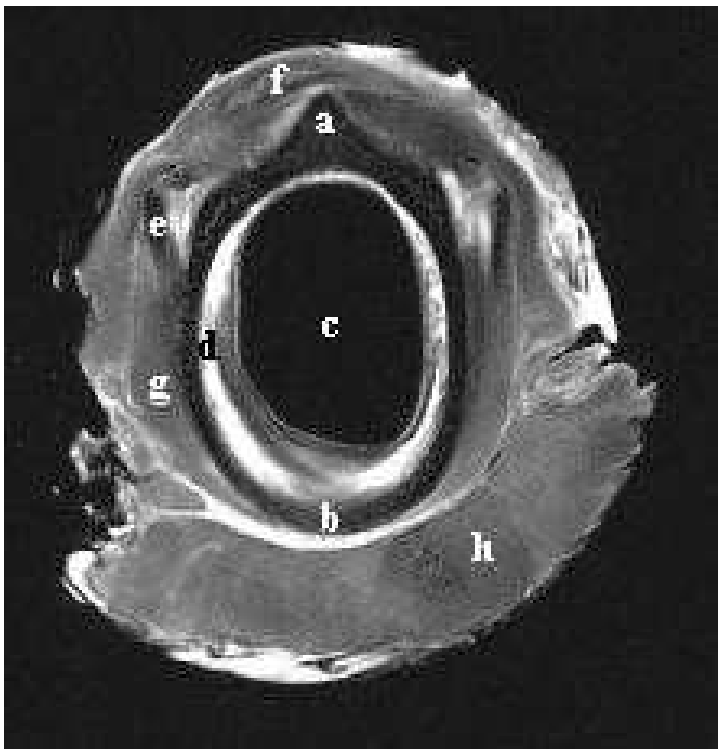

Figure 4: *ex vivo*

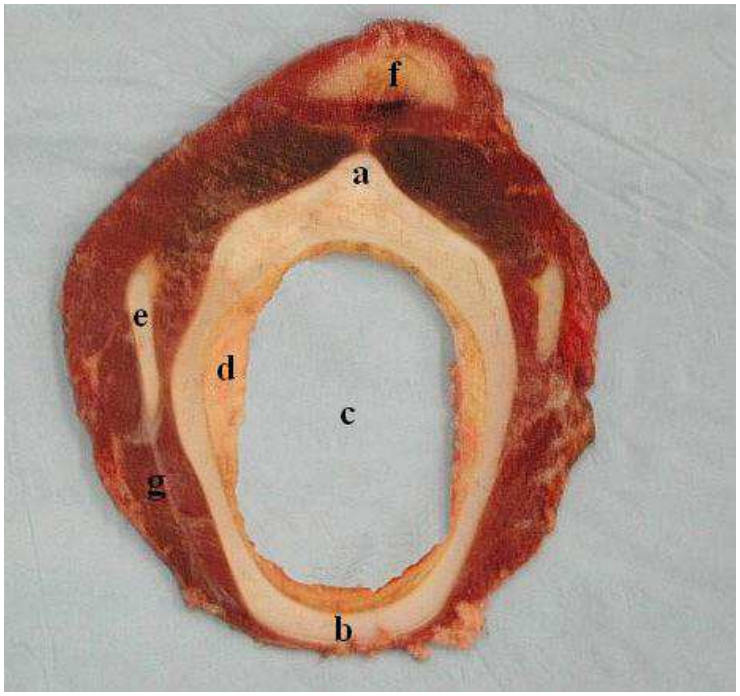

Figure 5: *ex vivo*

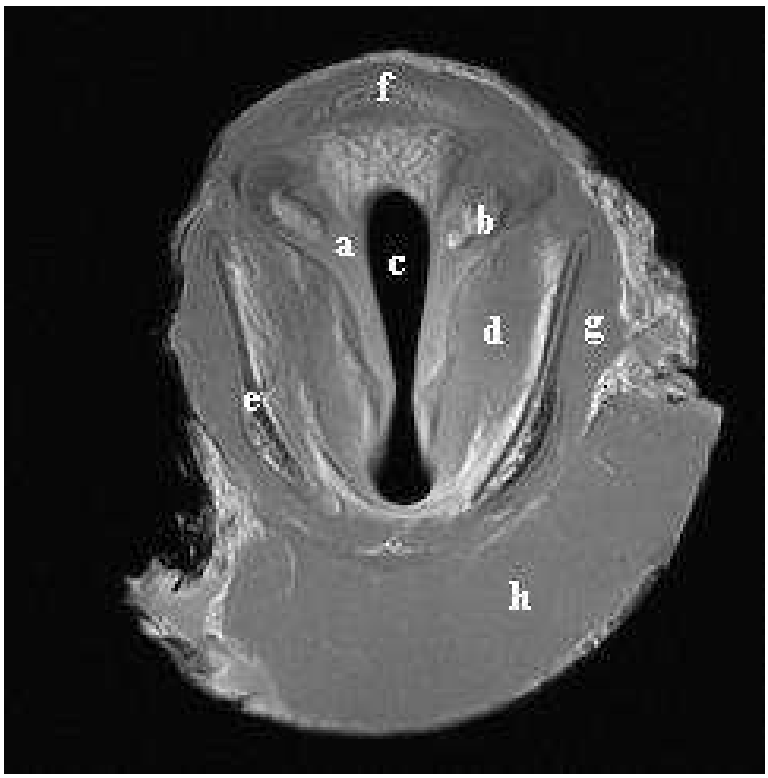

Figure 6: *ex vivo*

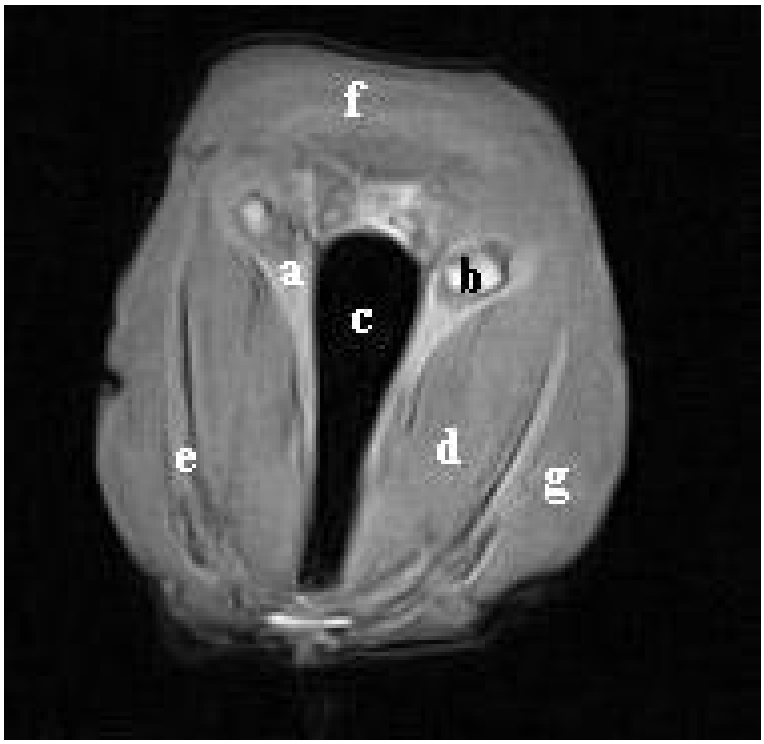

Figure 7: *ex vivo*

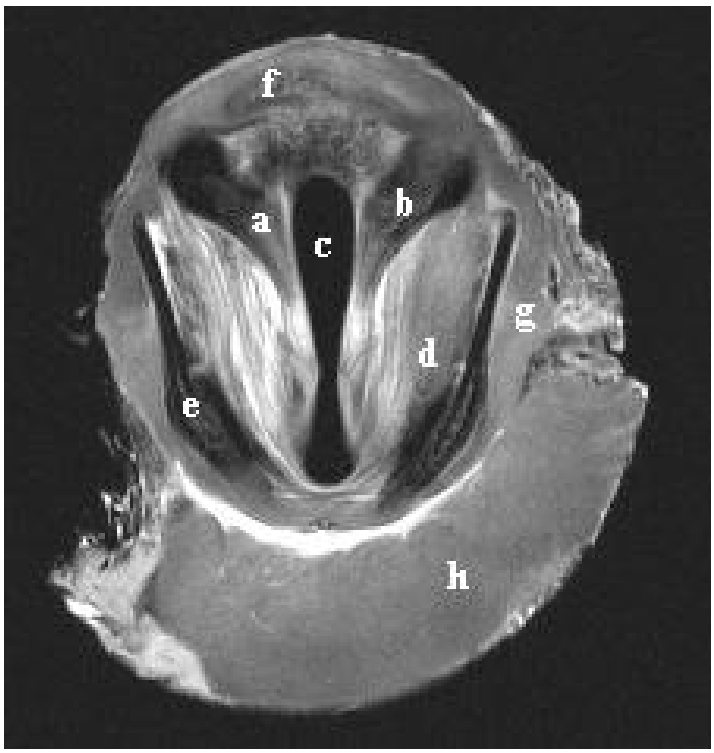

Figure 8: *in situ*

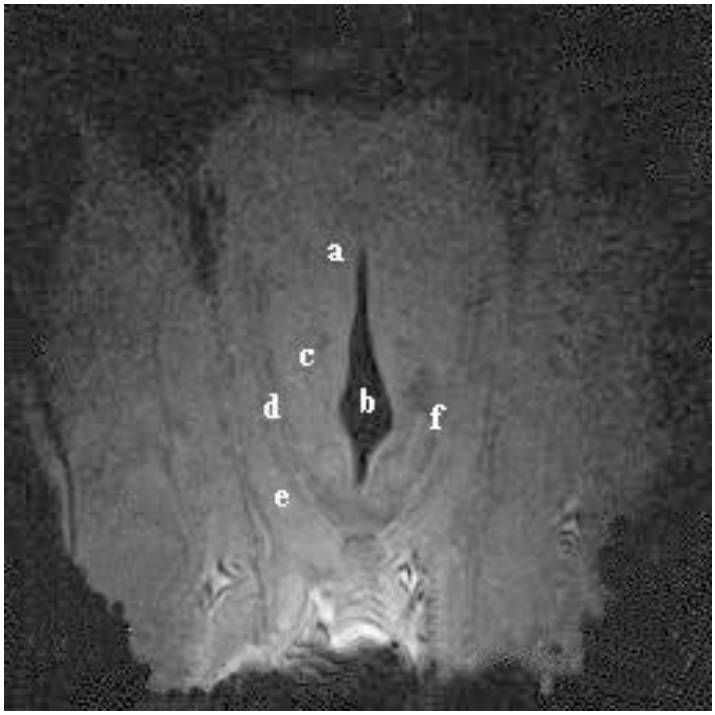

Figure 9: *ex vivo*

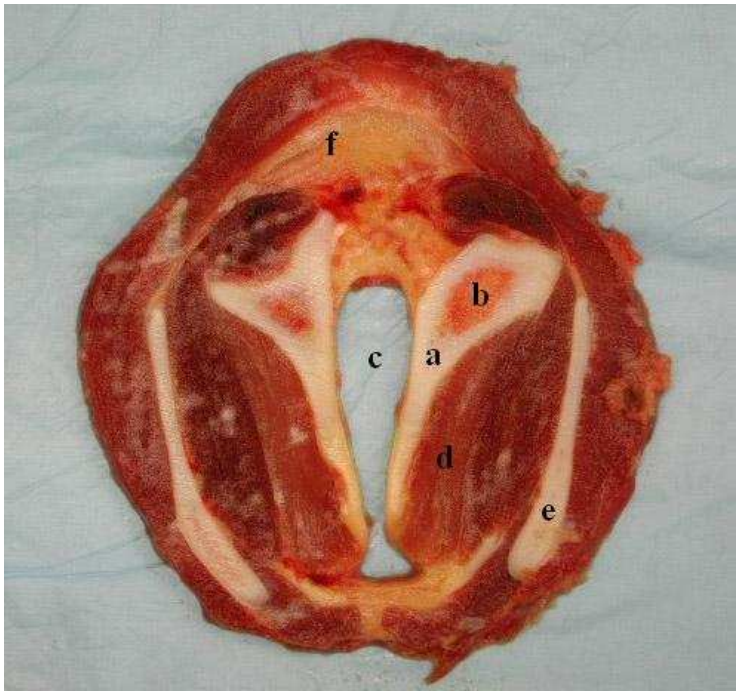

Figure 10: *ex vivo*

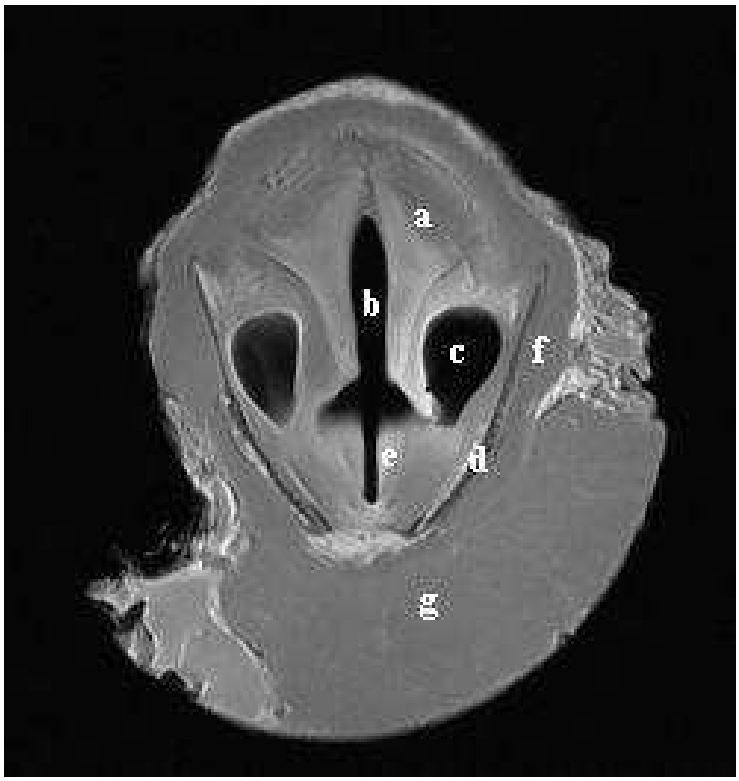

Figure 11: *ex vivo*

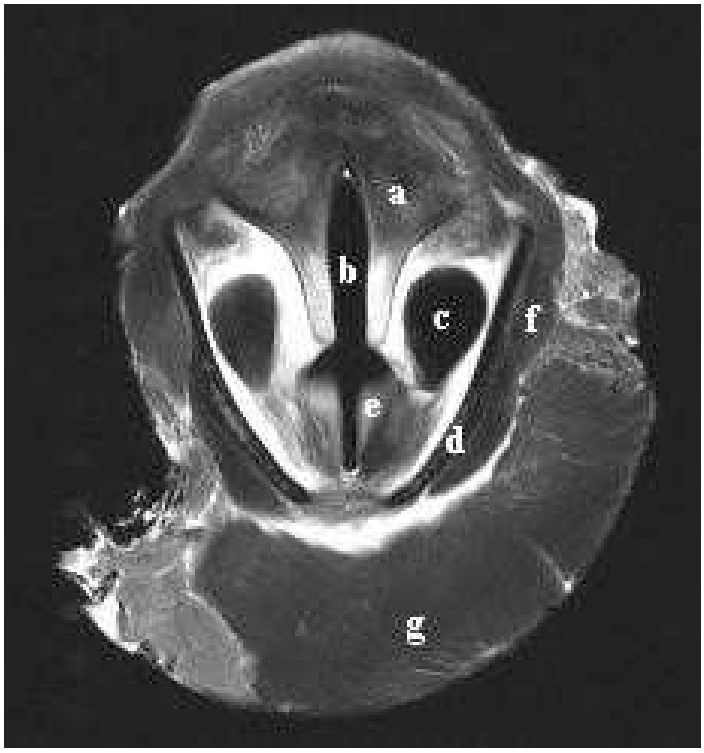

Figure 12: *ex vivo*

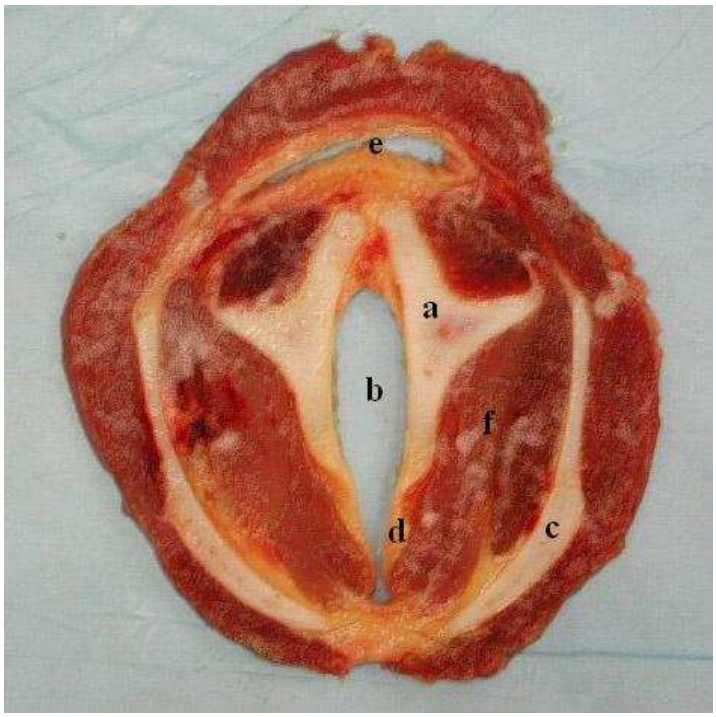

Figure 13: *ex vivo*

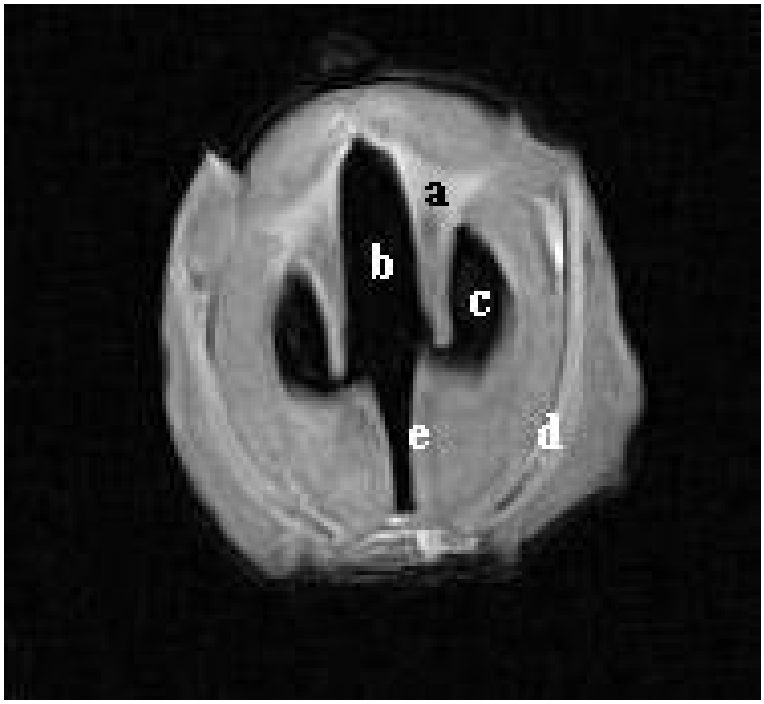

Figure 14: *in situ*

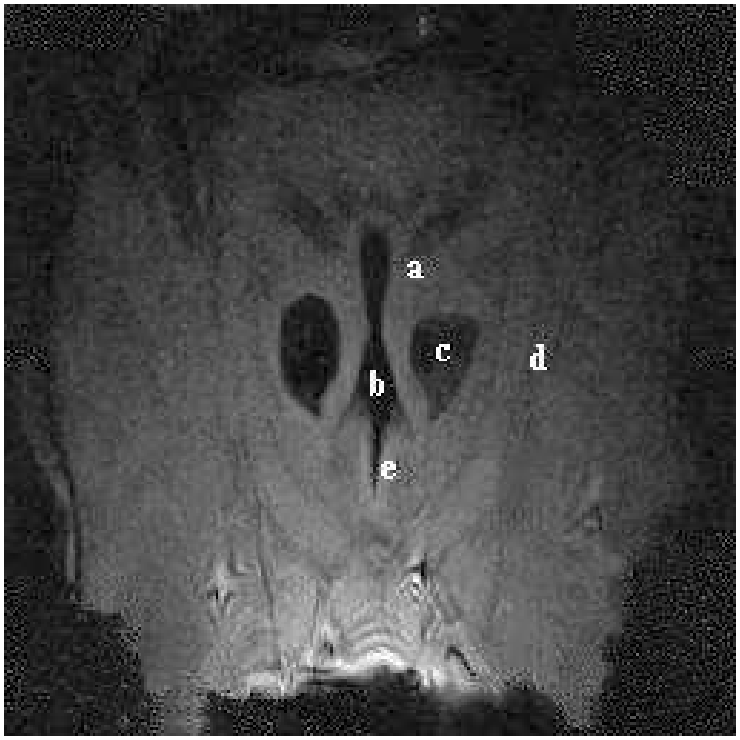

Figure 15: *ex vivo*

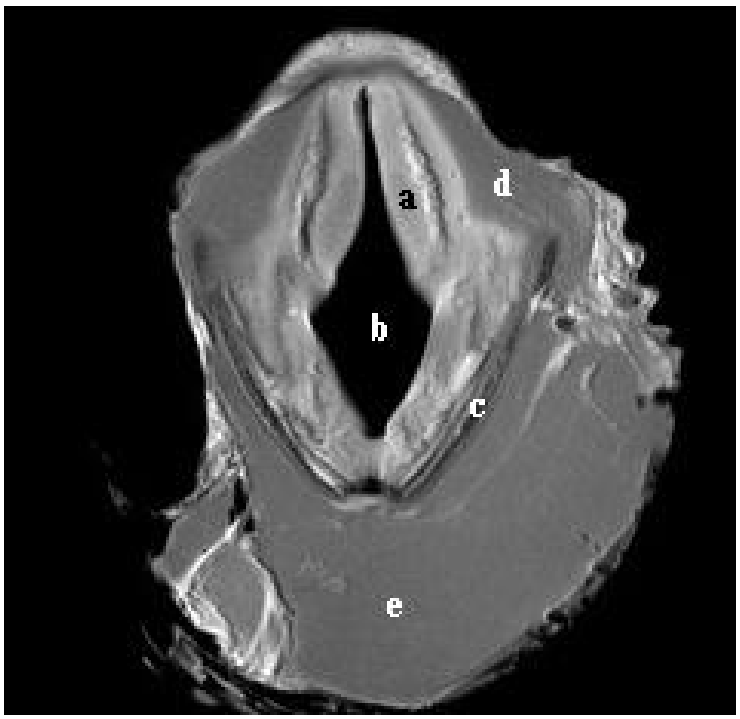

Figure 16: *ex vivo*

Figure 17: *ex vivo*

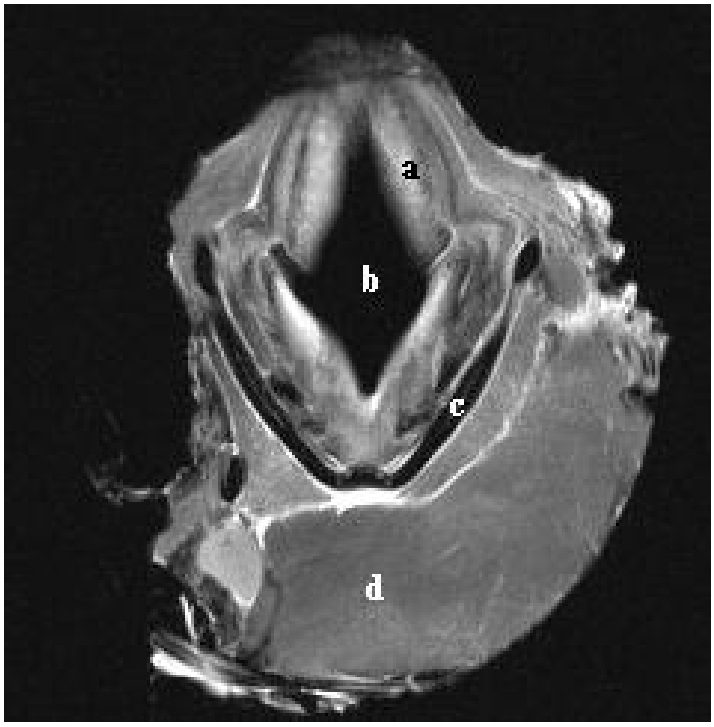

Figure 18: *ex vivo*

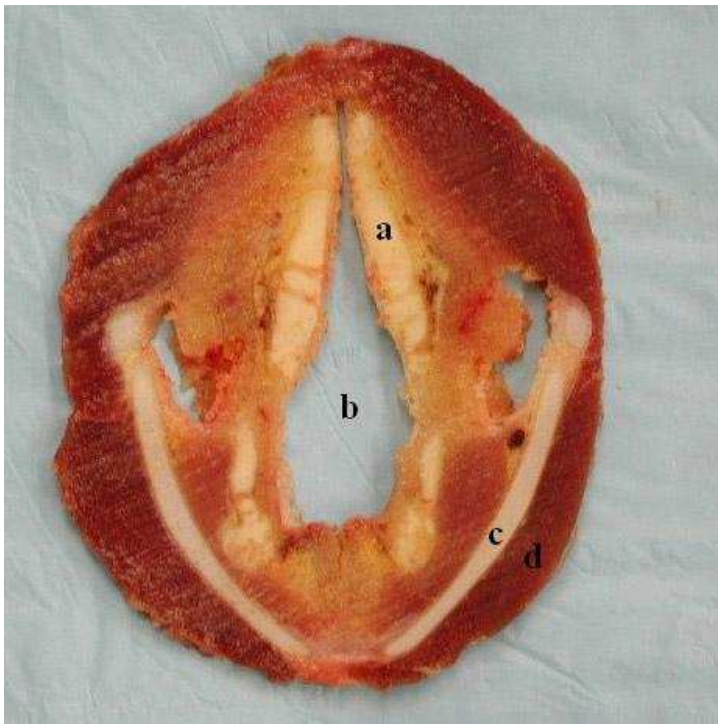

CONCLUSION

The 1.5 Tesla Siemens horizontal long-bore Vision-Sonata[b] MRI system was found to produce the highest subjective level of anatomical resolution. The 0.3 Tesla Hallmarq Equiscan 3000 [a] allowed imaging of the larynges *in situ* and was the most relevant to clinical equine practice. Differentiation and resolution of normal anatomical structures was subjectively superior with T1-weighted spin echo imaging sequences. T2-weighted sequences and inversion recovery (TIRM and STIR) sequences were found to be very similar in the images produced. Compared to the T1-weighted spin echo sequences, they offered improved tissue contrast. The equine larynges were represented by MRI imaging due to the density of tissue hydrogen present. MR imaging of the larynges was predictable and consistent in signal intensity based on the tissue composition and had excellent correlation with gross anatomic specimens. In summary, MRI was determined to be an effective, noninvasive means for evaluation of the internal morphology of the equine larynges. The technique will be useful in the clinical setting in determining extent and severity of equine laryngeal pathology in such conditions as arytenoid chondritis.